Effect of Favorable Pressure Gradients on Turbulent Boundary Layers

Large favorable pressure gradients can cause the drag of a turbulent boundary layer on a solid surface to decrease; if large enough, such gradients can cause a return to laminar flow. Scaling relations and a computational model for the viscous wall layer, recently developed in this laboratory are used to interpret this phenomenon.

D. S. Finnicum, T. J. Hanratty
Department of Chemical Engineering
University of Illinois
Urbana, IL 61801

Introduction

A large literature now exists for turbulent flows along flat surfaces in the presence of favorable pressure gradients. The motivation for these studies is the finding that drag decreases and that, for large enough pressure gradients, laminarization occurs. This paper uses a conceptual and computational model of turbulence close to a wall, recently developed by Nikolaides (1984), to provide a better understanding of the scaling and of the physics of this phenomenon.

It is generally accepted that the principal influence of pressure gradients on the turbulence is in the region close to the wall called the viscous wall region. The thickness of this region, y_o, made dimensionless with the kinematic viscosity ν, and a friction velocity defined with the wall shear stress u^*, is $y_o^+ = 30$–40 for a zero pressure gradient flow. The decrease of drag in a favorable pressure gradient can be associated with an increase in y_o^+.

Considerable attention has been given to structural aspects of the viscous wall region because it is believed they play a key role in understanding how turbulence is generated at a wall. The feature that has been of most interest is the existence of "organized" eddies, attached to the wall, that are elongated in the flow direction and have a dimensionless spanwise wavelength of $\lambda^+ = \lambda u^*/\nu \simeq 100$ in a zero pressure gradient. These eddies bring high-momentum fluid to the wall and eject low-momentum fluid from the wall (Hogenes and Hanratty, 1982). Tracer studies reveal that the ejection sometimes can lead to a violent interaction with the outer flow, called a burst. The time interval between these bursts is $T_B^+ \simeq 100$ for a zero pressure gradient. Drag-reduction has been associated with a decrease in T_B^+ or with an increase in λ^+ (Fortuna and Hanratty, 1972; Eckelman et al., 1972).

A critical ingredient in the results to be presented is the definition of an effective pressure gradient $P_e^+(y^+)$ for the viscous wall region:

$$\tau^+ = 1 + P_e^+ y^+ \tag{1}$$

For a Couette flow $P_e^+ = P^+$, where

$$P^+ = \frac{\nu}{\rho u^{*3}} \frac{d\bar{P}}{dx} \tag{2}$$

For an accelerating flow (in a favorable pressure gradient) part of the pressure gradient can be absorbed by inertia changes in the fluid so that the magnitude of P_e^+ is less than the magnitude of P^+. From Eq. 1 it is seen that the effective pressure gradient evaluated at y_o, P_{eo}^+, is related to the variation of the shear stress through the viscous wall region.

$$\frac{\tau_o}{\tau_w} = 1 + P_{eo}^+ y_o^+ \tag{3}$$

In this paper Nikolaides' scaling arguments are used to develop relations between λ^+, T_B^+, y_o^+, and P_{eo}^+ (or τ_o/τ_w). It is found that there is a minimum value of P_{eo}^+ for which the scaling relations can be satisfied. It is argued that this condition closely corresponds to where laminarization begins. The principal physical effects of a large favorable pressure gradient are the large variation of shear stress in the viscous wall region and the large direct transfer of energy from the pressure gradient to the turbulence. The 2½ D computational model developed by Nikolaides (1984) is used to determine how these effects alter the turbulent velocity field.

Scaling of the Viscous Wall Region

Scaling relations

It is assumed that the outer edge of the viscous wall region, y_o, resides in the log-layer. This outer edge is defined as a location where viscous transfer of momentum becomes negligible com-

Correspondence concerning this paper should be addressed to T. J. Hanratty.

pared to turbulent transfer. Consequently, a natural choice for y_o for all levels of acceleration is the distance from the surface where the ratio of the viscous stress to the total stress is equal to some small constant a_2:

$$\frac{\text{Viscous shear stress}}{\text{Total shear stress}} = \frac{\mu d\bar{U}/\text{dy}}{\tau}\bigg|_{y-y_o} = a_2 \tag{4}$$

For the zero pressure gradient case, where the shear stress in the log-layer is equal to the wall shear stress, dimensional reasoning and experimental results give

$$\frac{d\bar{U}}{dy} = \frac{\sqrt{\tau_w/\rho}}{\kappa y} \tag{5}$$

where $\kappa = 0.41$ is the von Karman constant. Townsend (1961) generalized this result for cases where the shear stress varies with y:

$$\frac{d\bar{U}}{dy} = \frac{\sqrt{\tau/\rho}}{\kappa y} \tag{6}$$

If Eq. 6 is substituted into Eq. 4 the following relation for y_o is obtained:

$$\frac{y_o\sqrt{\tau_o/\rho}}{\nu} = \frac{1}{\kappa a_2} = y_o^o \tag{7}$$

Here constant y_o^o is chosen as 40 to be consistent with results where τ at y_o equals τ_w. Thus $a_2 = 1/16.4$. It should be noted that Eq. 7 is the same as the suggestion by Launder and Jones (1969) that at the edge of the viscous wall layer the turbulent Reynolds number takes on a constant value.

An established property of the log-layer is that the production of turbulent energy, $-\overline{uv}\,d\bar{U}/dy$, is approximately equal to the rate of dissipation of turbulent energy, designated as ϵ (Townsend, 1976, p. 138; Hinze, 1975, pp. 649, 737; Bradshaw, 1976, p. 36). Therefore, since y_o is assumed to be at the inner edge of the log-layer,

$$\left(-\overline{uv}\frac{d\bar{U}}{dy}\right)_{y-y_o} \cong (\epsilon)_{y-y_o} \tag{8}$$

Outside the viscous wall layer an inviscid estimate can be made for the dissipation which Tennekes and Lumley (1972, p. 21) call one of the cornerstone assumptions of turbulence theory:

$$\epsilon = a_1\frac{q^3}{\ell} \tag{9}$$

where $q^2 = \overline{u^2} + \overline{v^2} + \overline{w^2}$ and ℓ is a characteristic length of the large eddies. In applying Eq. 9 to wall turbulence it follows that in the log-layer, ℓ varies linearly with distance from the wall and equals the Prandtl mixing length (Bradshaw, 1976, p. 37). This can be seen by substituting Eq. 6 into Eq. 8. The resulting equation is satisfied at $y = y_o$ if

$$\ell = \kappa y_o \tag{10}$$

and

$$q_o = \left(\frac{1}{a_1}\right)^{1/3}(-\overline{uv})_{y-y_o}^{1/2} \tag{11}$$

By using Eq. 4, Eq. 11 is written as

$$q_o\Big/\left(\frac{\tau_o}{\rho}\right)^{1/2} = \frac{(1-a_2)^{1/2}}{a_1^{1/3}} = q_o^o \tag{12}$$

The picture presented for the organized wall eddy by Nikolaides suggests that its characteristic length in the spanwise direction, λ, is related to the distance in the z direction between zero crossings of the v or w velocity. For a Gaussian signal the zero crossing scale, defined as $\Lambda = \frac{1}{2}\pi N_o$ (where N_o is the frequency of the signal) is equal to the Taylor microscale, λ_g. Consequently, Nikolaides assumed that the wavelength of the wall eddies is roughly equal to the Taylor microscale at $y = y_o$; that is,

$$\lambda_g|_{y_o} = \lambda/2\pi \tag{13}$$

For an isotropic turbulence (Hinze, 1975, p. 219)

$$\epsilon = 15\nu\frac{\overline{u^2}}{\lambda_g^2} \tag{14}$$

This equation has also been used to define the Taylor microscale in anisotropic turbulence with $3\overline{u^2} = (\overline{u_1^2} + \overline{u_2^2} + \overline{u_3^2}) = q^2$ (Tennekes and Lumley, 1972, p. 66) By equating Eqs. 14 and 9 and substituting Eq. 13 for λ_g, it is found that

$$\left[\frac{\lambda\left(\frac{\tau_o}{\rho}\right)^{1/2}}{\nu}\right]^2 = \frac{20\kappa\pi^2}{a_1 q_o^o}y_o^o = (\lambda^o)^2 \tag{15}$$

To be consistent with measurements for zero pressure gradient the constant λ^o is taken to be equal to 100. Relation 15 is the same as the relations derived by Hinze (1975, p. 225) and by Tennekes and Lumley (1972, p. 67), if κy_o is substituted for ℓ. The justification usually adopted for applying Eq. 14 to shear flows is the assumption that small-scale eddies defining λ_g are isotropic, even though the large-scale turbulence is anisotropic. Errors in this assumption are not critical since Eq. 14 is used here only to obtain a scaling relation.

Again, from arguments presented by Nikolaides, the period T_B is obtained by assuming that at y_o where viscosity is not affecting the wall eddy, transient terms are of the same order as the convective terms in the Navier-Stokes equations:

$$\frac{\partial u_i}{\partial t} \sim u_j\frac{\partial u_i}{\partial x_j} \tag{16}$$

This can be true if

$$\frac{\sqrt{\tau_o/\rho}}{T_B} \sim \frac{\tau_o/\rho}{\lambda} \tag{17}$$

or, equivalently,

$$\frac{T_B(\tau_o/\rho)}{\nu} = \lambda^o \tag{18}$$

The following relations that describe the influence of favorable pressure gradients on parameters characterizing the viscous wall region are therefore derived:

$$y_o^+ = y_o^o \left(\frac{\tau_w}{\tau_o}\right)^{1/2} \tag{19}$$

$$q_o^+ = q_o^o \left(\frac{\tau_o}{\tau_w}\right)^{1/2} \tag{20}$$

$$\lambda^+ = \lambda^o \left(\frac{\tau_w}{\tau_o}\right)^{1/2} \tag{21}$$

$$T_B^+ = T^o \left(\frac{\tau_w}{\tau_o}\right) \tag{22}$$

with $y_o^o = 40$, $q_o^o = 2.72$, $\lambda^o = 100$, and $T^o = 100$.

It is noted that the parameter τ_o/τ_w, representing the shear stress variation in the viscous wall region, describes the influence of the pressure gradient. This can be calculated from Eq. 1 as

$$\frac{\tau_o}{\tau_w} = 1 + P_{eo}^+ y_o^o \left(\frac{\tau_w}{\tau_o}\right)^{1/2} \tag{23}$$

We have chosen to correlate y_o^+, q_o^+, λ^+, and T_B^+ vs. P_{eo}^+ (rather than τ_o/τ_w) in Figure 1. The interesting aspect of these plots is that they show a minimum value of $P_{eo}^+ = -0.00962$ for which the scaling relations can be satisfied. At this minimum, $y_o^+ = 69.28$, $\lambda^+ = 173$, $T_B^+ = 300$, $\tau_o^+ = 0.333$, and $q_o^+ = 1.57$. The value of τ_o/τ_w (and P^+) decreases as one progresses to smaller P_{eo}^+ along the lower branches and to the larger P_{eo}^+ along the upper branches of the curves in Figure 1. The rapid increase in y_o^+ along the upper branch suggests that the log-layer disappears and that laminarization occurs with decreases of τ_o/τ_w at, or somewhat lower than, 0.333. Thus $P_{eo}^+ = -0.00962$ could represent a criterion for the approach to laminarization and the upper branches could be meaningless since they were calculated assuming that y_o is located in a log-layer.

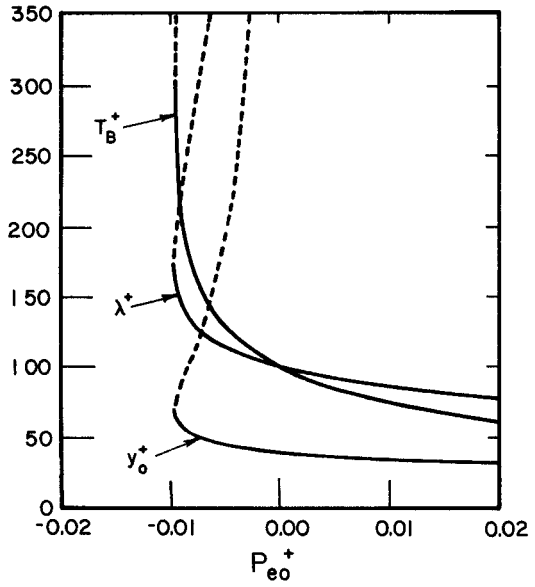

Figure 1. Variation of streak spacing, bursting period, and edge of viscous wall layer with P_{eo}^+.

Comparison of scaling relations with measurements

Parameters used in the literature to represent the effect of pressure gradient on turbulent boundary layers are

$$K = \frac{\nu}{U_\infty^2}\frac{dU_\infty}{dx} \tag{24}$$

and

$$P^+ = \frac{\nu}{\rho u^{*3}}\frac{d\bar{P}}{dx} \tag{25}$$

Therefore, in order to compare the scaling relations developed in the previous section it is necessary to relate P_{eo}^+ to these parameters. This is accomplished by using the following relation developed by Julien et al. (1969) and Loyd et al. (1970) for asymptotic similar sink flows for the region $y^+ < 150$:

$$\tau^+ = 1 + P^+ y^+ \left(1 - \frac{C_f}{2}\frac{1}{y^+}\int_0^{y^+} \bar{U}^{+2}\, dy^+\right) \tag{26}$$

From Eq. 24,

$$P_{eo}^+ = P^+\left(1 - \frac{C_f}{2}\int_o^{y_o^+} \bar{U}^{+2}\, dy^+\right) \tag{27}$$

Experimental data for $C_f/2 = \tau_w/\rho\bar{U}_\infty^2$ for asymptotic boundary layers are given in Figure 2. These along with $\bar{U}^+(y)$ calculated with the computational model discussed later are used to relate P^+ and K^+ to P_{eo}^+.

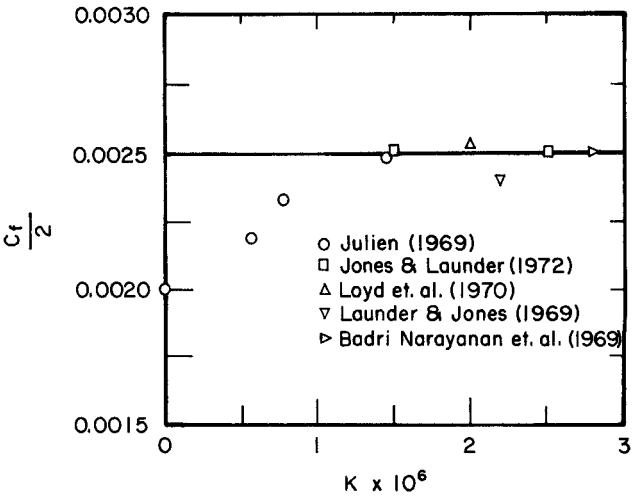

Figure 2. Skin friction coefficient data of several investigators.

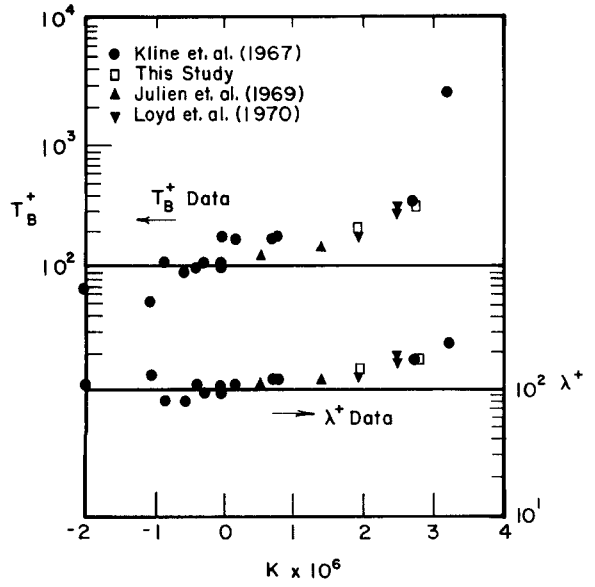

Figure 3. Streak spacings and bursting periods.
Results obtained using the scaling arguments and mean velocity profiles of several investigators

Comparisons of the calculated effects of K^+ on λ^+ and T_B^+ with measurements are given in Figure 3. Good agreement is noted.

Comparison of scaling relations with laminarization results

It is of interest to compare the minimum $P_{eo}^+ = -0.00962$ with experimental criteria for laminarization. Again, by using the calculated velocities presented in the next section and Eq. 27, it is found that $P_{eo}^+ = -0.00962$ corresponds to $K^+ = 2.8 \times 10^{-6}$ and $P^+ = -0.0225$. These compare favorably with the experimental values of $2.5 \times 10^{-6} \geq K^+ \geq 3.5 \times 10^{-6}$ and of $-0.02 \geq P^+ \geq -0.025$. (Launder, 1963, 1964; Kline et al., 1967; Moretti and Kays, 1965; Launder and Stinchcombe, 1967; Back and Seban, 1967; Loyd et al., 1970; Jones and Launder, 1972; Patel, 1965; Badri Narayanan and Ramjee, 1969.

Patel and Head (1968) suggest $\Delta_\tau^+ = (\nu/\rho u^{*3})(d\tau/dy)$ as a criterion for laminarization. They approximated the variation of τ^+ in the wall region with a linear relation and suggested from experimental measurements that $\Delta_\tau^+ = -0.009$. It is to be noted that at the minimum of P_{eo}^+, $(d\tau^+/dy^+)_o = P_{eo}^+ = -0.00962$. Furthermore, from the calculated values of $\tau_o/\tau_w = 0.333$ and of $y_o^+ = 69.28$ it is found that the scaling relations give $(\tau_o^+ - \tau_w^+)/y_o^+ = -0.00962$ for $P_{eo}^+ = -0.00962$. Thus the use of the minimum P_{eo}^+ as a criterion for laminarization is also consistent with the proposal of Patel and Head.

Computational Model

Review of previous work

Hatziavramidis and Hanratty (1979) explored a simple 2½D computational model to represent the time-varying velocity field in the viscous wall region. Use was made of the observation of elongated flow structures to assume that derivatives of hydrodynamic variables in the flow direction are negligible. The three velocity components were calculated in a plane perpendicular to the direction of mean flow by solving the unaveraged Navier-Stokes equations. The boundary conditions at y_o were represented by a velocity field homogeneous in the flow direction, periodic in the spanwise direction and in time with wavelength of $\lambda^+ = 100$ and period $T_B^+ = 100$. Statistical characteristics of the flow field, calculated from the Hatziavramidis model by averaging in time and in the spanwise direction for fixed y, are in good agreement with measurements for zero pressure gradient.

Nikolaides (1984) recognized that the boundary conditions used by Hatziavramidis and Hanratty are unrealistic in that they do not take account of the experimental evidence that eddies with larger spanwise wavelengths that $\lambda^+ = 100$ dominate the flow at y_o^+. He repeated the calculations using a velocity field that has two harmonics, $\lambda_1^+ = 100$, $T_1^+ = 100$ and $\lambda_2^+ = 400$, $T_2^+ = 400$. These provide a better representation of the variation of spanwise velocity fluctuations and of the dissipation of energy.

These calculations give the following physical picture. The viscous interaction with the wall is controlled by disturbances in the y-z plane, which are elongated in the flow direction with a wavelength of $\lambda^+ = 100$ for a flow with zero pressure gradient. These disturbances bring high-momentum fluid toward the wall, exchange momentum with the wall to create velocity-deficient fluid, and transport this velocity-deficient fluid away from the wall. The wall eddies, by this process, convert mean flow energy transported to the viscous wall region into large streamwise velocity fluctuations. This is manifested by the observed maximum in $\overline{u^2}$ at $y^+ \simeq 12$ and the finding that the calculated variation of $\overline{u^2}$ with y^+ close to the wall is independent of the streamwise velocity fluctuations imposed at y_o^+. The streamwise velocity fluctuations, created in the viscous wall layer, are converted into normal and spanwise fluctuations beyond $y_o^+ = 40$, through a correlation between fluctuations in the pressure and velocity derivatives in the flow direction. These, in turn, interact with the wall to repeat the cycle.

Description of computational model

This computational model of Nikolaides has been used to study the effect of favorable pressure gradients on turbulence properties of the viscous wall region. As mentioned above, the model makes use of the observation that turbulence scales in the flow direction are longer than in the spanwise and normal directions in the viscous wall region. The Navier-Stokes equations are, therefore, simplified by neglecting all derivatives in the x direction:

$$\frac{\partial v}{\partial t} + \frac{\partial (v^2)}{\partial y} + \frac{\partial (vw)}{\partial z} = -\frac{1}{\rho}\frac{\partial p}{\partial x} + \nu\left(\frac{\partial^2 v}{\partial y^2} + \frac{\partial^2 v}{\partial z^2}\right) \tag{28}$$

$$\frac{\partial w}{\partial t} + \frac{\partial (vw)}{\partial y} + \frac{\partial (w^2)}{\partial z} = -\frac{1}{\rho}\frac{\partial p}{\partial z} + \nu\left(\frac{\partial^2 w}{\partial y^2} + \frac{\partial^2 w}{\partial z^2}\right) \tag{29}$$

$$\frac{\partial U}{\partial t} + \frac{\partial (vU)}{\partial y} + \frac{\partial (wU)}{\partial z} = -\frac{d\tau}{dy} + \nu\left(\frac{\partial^2 U}{\partial y^2} + \frac{\partial^2 U}{\partial z^2}\right) \tag{30}$$

$$\frac{\partial w}{\partial z} + \frac{\partial v}{\partial y} = 0 \tag{31}$$

where $U = \overline{U} + u$ and

$$\frac{d\tau}{dy} = \frac{1}{\rho}\frac{\partial \overline{P}}{\partial x} + \overline{U}\frac{\partial \overline{U}}{\partial x} + \overline{V}\frac{\partial \overline{U}}{\partial y} \tag{32}$$

It is noted that the assumption of homogeneity in the streamwise direction decouples the v and w equations from the U equation, which makes numerical solution of Eqs. 28–32 easier.

Equations 28–32 are solved using the boundary conditions

$$U = v = w = 0 \quad \text{at } y = 0$$

$$w = 0, \quad \frac{\partial v}{\partial z} = 0, \quad \frac{\partial w}{\partial z} = 0 \quad \text{at } z = 0, \quad z = z_o$$

where $z_o = \lambda_2/2$. The upper boundary of the computational domain is located at the outer edge of the viscous wall region, y_o, where the velocities are specified as follows:

$$w = \hat{w}_1 \cos\left(\frac{2\pi t}{T_1} + \Phi_{w1}\right) \sin\left(\frac{2\pi z}{\lambda_1}\right) + \hat{w}_2 \cos\left(\frac{2\pi t}{T_2} + \Phi_{w2}\right) \sin\left(\frac{2\pi z}{\lambda_2}\right) \quad (33)$$

$$v = \hat{v}_1 \cos\left(\frac{2\pi t}{T_1} + \phi_{v1}\right) \sin\left(\frac{2\pi z}{\lambda_1}\right) + \hat{v}_2 \cos\left(\frac{2\pi t}{T_2} + \Phi_{v2}\right) \sin\left(\frac{2\pi z}{\lambda_2}\right) \quad (34)$$

$$U = \bar{U}(y_o) + \hat{u}_1 \cos\left(\frac{2\pi t}{T_1} + \Phi_{u1}\right) \sin\left(\frac{2\pi z}{\lambda_1}\right) + \hat{u}_2 \cos\left(\frac{2\pi t}{T_2} + \Phi_{u2}\right) \sin\left(\frac{2\pi z}{\lambda_2}\right) \quad (35)$$

The components with λ_1 and T_1 scales are associated with the wall eddies, while the components with λ_2 and T_2 scales reflect the contribution of the outer flow eddies to the dynamics of the viscous wall region.

It should be noted that the specification of w and v at y_o also amounts to the specifications of v at the first grid points from y_o since the finite-difference scheme requires that conservation of mass, Eq. 31, be satisfied. The possibility of using conservation of mass directly in the boundary conditions was also considered. This would have required the specification of $\partial v/\partial y$ at y_o rather than v. This was not pursued because of anticipated numerical difficulties, and because it was felt that the accurate specification of v at y_o is critically important. Present experimental results suggest that the v velocity is the most energetic $\lambda^+ \approx 100$ component at y_o and that the $\lambda^+ = 100$ eddies at the wall are associated more strongly with the v velocity component at y_o than with the w component.

The principal influences of a favorable pressure gradient according to the computational model are the changes in the specification of the amplitudes and scales in Eqs. 33–35 caused by the large change in τ through the viscous wall region and the appearance of $d\tau/dy$ in Eq. 32. For a zero pressure gradient this term is zero. For the favorable pressure gradient case $-d\tau/dy$ is a positive momentum source term that causes variations of u in the y, z plane.

If the advective terms on the righthand side of Eq. 32 are negligible,

$$\tau^+ = 1 + P^+ y^+ \quad (36)$$

Experiments by Sandborn and Slogar (1955) and by Bradshaw (1969) show that acceleration within the viscous wall region cannot be neglected and that Eq. 36 is incorrect for flows with high favorable pressure gradients. The special case of an asymptotic similar sink flow is assumed so that the variation of τ^+ with y^+ is calculated from Eqs. 1, 26, and 27. Thus

$$\frac{d\tau^+}{dy^+} = P^+ \left(1 - \frac{C_f}{2} \bar{U}^{+2}\right) \quad (37)$$

and

$$P_e^+ = P^+ \left(1 - \frac{C_f}{2} \frac{1}{y^+} \int_o^{y^+} \bar{U}^{+2}\, dy^+\right) \quad (38)$$

Specifications of the flow at y_o

The principal theoretical problem in using this 2½D model is the specification of the parameters in the boundary conditions, Eqs. 33–35. The conditions used by Nikolaides for a zero pressure gradient are as follows

$$y_o^+ = 40$$

$$T_1^+ = \lambda_1^+ = 100$$

$$T_2^+ = \lambda_2^+ = 400$$

$$E_{u_1} = \hat{u}_1/(\hat{u}_1 + \hat{u}_2) = 0.15$$

$$E_{v_1} = \hat{v}_1/(\hat{v}_1 + \hat{v}_2) = 0.75$$

$$E_{w_1} = \hat{w}_1/(\hat{w}_1 + \hat{w}_2) = 0.40$$

$$\Phi_{u1} = 216^0 \quad \Phi_{v1} = 36^0 \quad \Phi_{w1} = 0^0$$

$$\Phi_{u2} = 194.4^0 \quad \Phi_{v2} = 90^0 \quad \Phi_{w2} = 270^0$$

These parameters were chosen to agree with presently available measurements of the velocity field at $y_o^+ \simeq 40$ for a zero pressure gradient case. The detailed reasoning behind their choice may be found in the thesis of Nikolaides (1984). Good agreement between the calculated and measured velocity fields and between calculated and measured energy balance relations was obtained with the above choice of parameters.

As might be guessed, there is some leeway in the choice because of the lack of information about the exact flow behavior at y_o. For example, the representation of all large-scale motions with $\lambda_2^+ = 400$ is a simplication, but the calculated results are not very sensitive to the selection of λ_2^+. However, in varying these parameters characterizing the flow behavior at $y_o^+ = 40$ certain criteria had to be satisfied to be consistent with established experimental results. The total $\overline{u^2}$, $\overline{v^2}$, and $\overline{w^2}$ energies at y_o^+ had to agree with measurements. The specification of E_{u_1}, E_{w_1}, and E_{v_1} had to be consistent with the observation that most of the energy of the v component and very little of the energy of the u component is associated with $\lambda^+ = 100$ wavelengths at $y_o^+ = 40$. The phase angle Φ_{v1} was chosen so that λ_1 eddies were closed for $o < y^+ < 40$ and open for $o < y^+ < 20$ most of the time. The phases $\Phi_{u1} - \Phi_{v1}$ and $\Phi_{u2} - \Phi_{v2}$ were chosen so as to correctly specify the Reynolds stress at $y_o^+ = 40$. Phase difference

$\Phi_{v2} - \Phi_{w2}$ was chosen so that the λ_2 eddies are open all the time. The value $\overline{U}_o^+$ was adjusted so that $\overline{U}^+ = y^+$ for $y^+ \to o$.

In order to use this model to examine the effect of favorable pressure gradients it is necessary to address the question of how the boundary conditions change from those specified for the zero pressure gradient case.

Badri Narayanan and Nerasimha (1974) showed that the Reynolds stress correlation stays roughly constant at about 0.5 in both accelerated and nonaccelerated flows. This constancy of the Reynolds stress correlation at y_o^+ was also observed in experiments of Nyden (1985). This information is used to support the assumption that the phase angles and the relative energies of u and v are independent of the acceleration. Thus variations in the Reynolds stress reflect variations in amplitudes of the fluctuating velocities. Jones and Launder (1972) also found that the intensities of the different turbulent velocity components in a flow with a large favorable pressure gradient are roughly in the same proportion to each other as in a nonaccelerated flow and that the intensity levels are set by the local shear stress. Therefore, it is assumed that all the amplitudes in Eqs. 33–35 change by the same fraction, given by Eq. 20, in an accelerating flow. Furthermore, it is assumed that λ_1^+, T_1^+ are given by Eqs. 21 and 22, and that the ratios λ_2/λ_1, T_2/T_1 are the same as for the nonaccelerating flow.

Some other minor changes were made in the boundary conditions used by Nikolaides for the zero pressure gradient case so as to give a better fit to the following equations for the mean velocity and the velocity gradient at y_o:

$$\overline{U}^+ = 2.44 \ln y^+ + 5 \tag{39}$$

$$\frac{d\overline{U}^+}{dy^+} = \frac{2.44}{y^+} \tag{40}$$

These involved changing $Ev_1 = \hat{v}_1/(\hat{v}_1 + \hat{v}_2)$ from 0.75 to 0.70, $Ew_1 = \hat{w}_1/(\hat{w}_1 + \hat{w}_2)$ from 0.40 to 0.37, and the phase Φ_{u_2} from 194.4 to 196 degrees.

Numerical methods

Calculations were done for a fixed P_{eo}^+ or a fixed y_o^+. The stream function-vorticity formulations of Eqs. 28 and 29 were solved numerically with the alternating direction implicit scheme to evaluate v and w. Details may be found in a thesis by Finnicum (1986).

An iterative procedure had to be used to calculate U from Eq. 30 since $\overline{U}^+(y)$ had to be known to specify P^+ or $d\tau^+/dy^+$ (see Eqs. 37 and 38). Also, during the iteration procedure slight adjustments were made in $\overline{U}^+$ at y_o so that the Couette flow relation

$$\overline{U}^+ = y^+ + P^+ y^{+2}/2 \tag{41}$$

was exactly satisfied for $y^+ \to 0$.

It is noted from Eqs. 37 and 38 that the friction coefficient has to be known to calculate P^+ and $d\tau^+/dy^+$ from the specified P_{eo}^+. The computational model does not calculate $C_f/2$ since it considers only $0 < y^+ < y_o^+$. Consequently the experimental results in Figure 2 were used. Here the acceleration is expressed in terms of the group K defined by Eq. 24. It is seen that for K values greater than 1.5×10^{-6} ($P^+ < -0.012$), $C_f/2$ is constant and equal to 0.0025. Stronger accelerations than about $K = 2.8 \times 10^{-6}$ cause relaminarization of the boundary layer. This is associated with a drop of $C_f/2$ to the accelerated laminar value, which can be determined analytically (Launder and Stinchcombe, 1967) as

$$C_f/2 = 1.155\, K^{1/2} \tag{42}$$

For example, an accelerated boundary layer, with $K = 2.8 \times 10^{-6}$, that is undergoing relaminarization will have its skin friction coefficient decrease from 0.0025 to 0.00193.

To test the spatial resolution of the program, the number of grid points in the y direction was increased from 51 to 101, and in the z direction from 101 to 201. The fourth-order moments calculated for a nonaccelerated flow were found to be equivalent to six significant figures. Therefore, all the calculations were done with a 51 × 101 grid. The time step used was $\Delta t^+ = 0.333$.

Results of Numerical Calculations

Conditions for the calculations

Calculations were done for three values of y_o^+. These correspond to a nonaccelerated flow ($P_{eo}^+ = 0$, $y_o^+ = 40$), a flow with a large favorable pressure gradient ($P_{eo}^+ = -0.0096$, $K = 2.8 \times 10^{-6}$, $y_o^+ = 69.3$), and a flow with a moderate favorable pressure gradient ($P_{eo}^+ = -0.0087$, $K = 2.03 \times 10^{-6}$, $y_o^+ = 56.0$).

Average properties were calculated at a fixed distance from the wall after the calculations reached a stationary state. This was done by averaging in time and in the z direction. A comparison of the calculations with the measurements for the zero pressure gradient case has already been made by Nikolaides (1984). The main focus of this presentation will therefore be to examine the effect of favorable pressure gradients.

Calculated statistical properties

Figure 4 shows calculated mean velocities. The dash-dot curve is the laminar sink flow solution of Pohlhausen (1921) that, as pointed out by Launder and Stinchcombe, would be

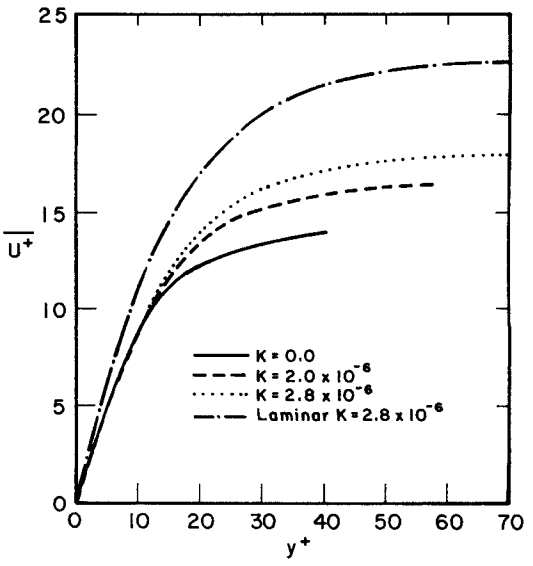

Figure 4. Calculated mean velocity profiles.

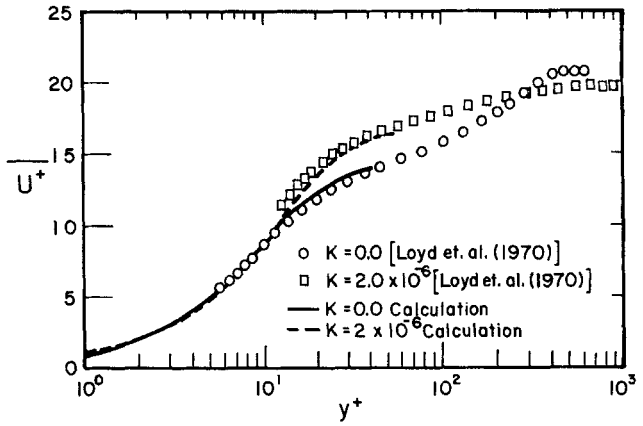

Figure 5. Mean velocity profiles, calculated and experimental.

obtained after the relaminarization of a flow with a pressure gradient just greater than $P^+ = -0.0225$.

In the viscous wall layer ($y^+ < 6$), velocities for the accelerated flows are slightly less than for the nonaccelerated flow. This is because the velocity profile has to satisfy Eq. 36 for $y^+ \to 0$. As the imposed pressure gradient increases, the velocity profile outside the viscous wall layer increases toward the laminar value, indicating that the flow is becoming less turbulent. The results in Figure 4 agree with Eq. 6, which predicts that the slope of the mean velocity profile at y_o^+ should be lower in favorable pressure gradients, since τ_o^+ is lower and y_o^+ is higher. These trends are in agreement with experimental results found in the literature (Jones and Launder, 1972). Mean velocity data of Loyd et al. (1970) for $K = 0$ and $K = 2 \times 10^{-6}$ are compared with calculated profiles in Figure 5. Good agreement is observed.

Calculated u intensity profiles are presented in Figure 6. Increasing the favorable pressure gradient has the effect of moving the peak of the profile away from the wall and of slightly

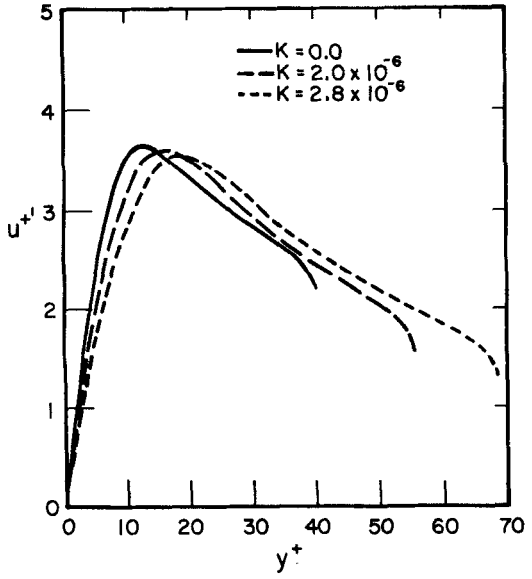

Figure 6. Calculated intensities of streamwise velocity fluctuations.

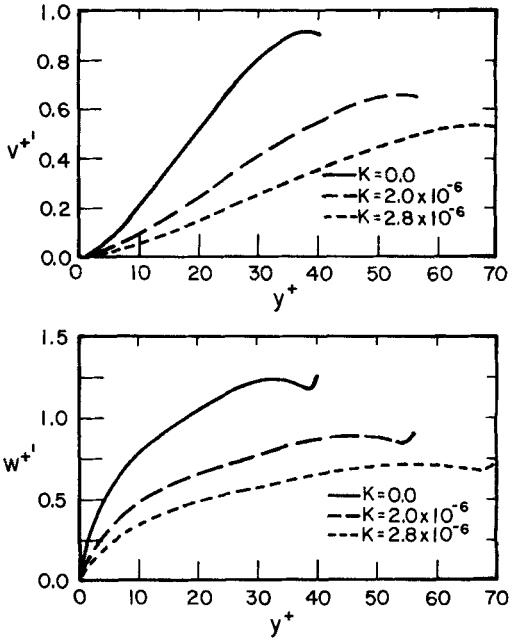

Figure 7. Calculated intensities of normal and spanwise velocity fluctuations.

lowering the maximum value. Figure 7 shows the v and w intensity profiles. In contrast to the u intensity profile, there is a dramatic decrease in the fluctuations throughout the viscous wall region as the imposed pressure gradient is increased. The Reynolds stress, shown in Figure 8, also shows a dramatic decrease in amplitude.

These results agree with experimental data (Jones and Launder, 1972; Launder and Stinchcombe, 1967; Badri Narayanan and Ramjee, 1969) showing a high streamwise intensity at pressure gradients up to the relaminarization point. The data of Badri Narayana and Ramjee indicate that after relaminariza-

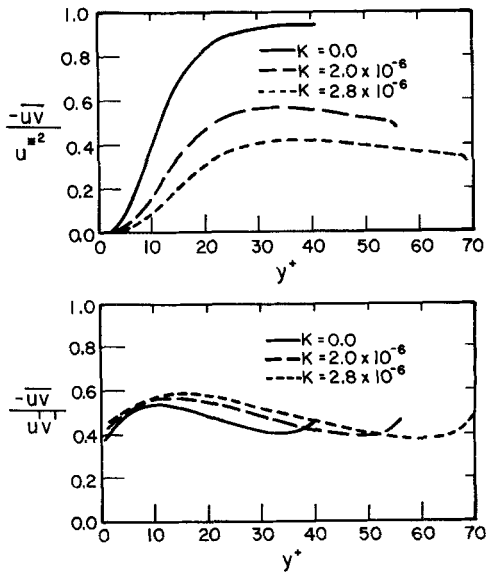

Figure 8. Calculated Reynolds stress and Reynolds stress correlations.

tion there is rapid decay of streamwise fluctuations until an essentially laminar flow remains.

Reynolds stress correlation results are also shown in Figure 8. No effect of pressure gradient is observed on the correlation of the Reynolds stress. This indicates that the decrease in the Reynolds stress is associated more with a reduction in the amplitude of the secondary motion than with a change in the basic processes involved.

Figure 9 shows the streamwise skewness and flatness profiles for the three cases. The large positive skewness near the wall is the result of inflows of high streamwise momentum close to the wall and the negative skewness is the result of ejections of low-momentum fluid. As seen in Figure 9, both quantities are roughly independent of pressure gradient.

The equation for the mean flow kinetic energy in a boundary layer is as follows:

$$\underset{\text{I}}{-\bar{U}\left(\bar{U}\frac{\partial \bar{U}}{\partial x}+\bar{V}\frac{\partial \bar{U}}{\partial y}\right)}\underset{\text{II}}{-\frac{\bar{U}}{\rho}\frac{\partial \bar{P}}{\partial x}}\underset{\text{III}}{-\frac{\partial(\overline{uv}\,\bar{U})}{\partial y}}+\underset{\text{IV}}{\overline{uv}\frac{\partial \bar{U}}{\partial y}}+\underset{\text{V}}{\nu\frac{\partial}{\partial y}\left(\bar{U}\frac{\partial \bar{U}}{\partial y}\right)}\underset{\text{VI}}{-\nu\left(\frac{\partial \bar{U}}{\partial y}\right)^2}=0 \quad (43)$$

Term II is the energy transferred directly to the mean flow by the pressure gradient. Term I is the energy used to accelerate the flow. Term VI is the direct viscous dissipation of mean flow energy into heat. Term IV is the dissipation of mean flow energy into turbulence. Term III is the turbulent transport of mean flow energy. Term V is the viscous transport of mean flow energy. To

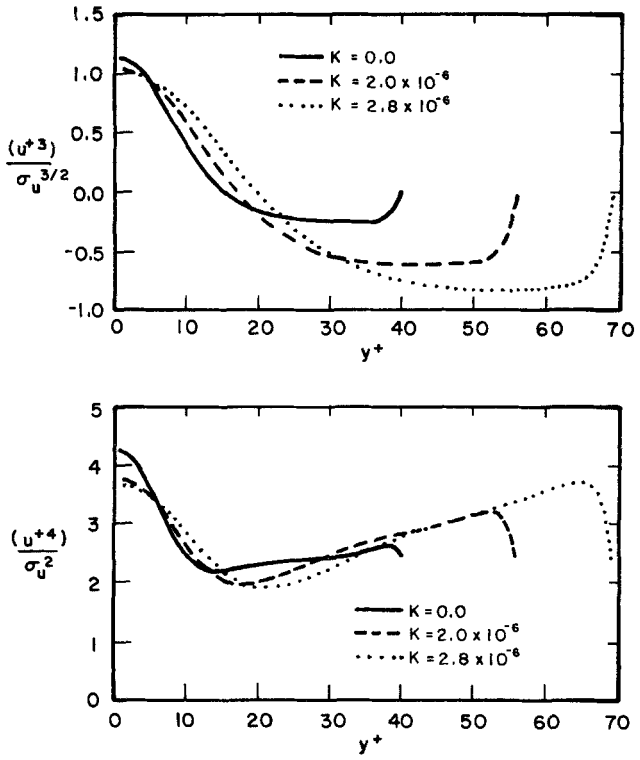

Figure 9. Calculated skewness and flatness factors of streamwise velocity component.

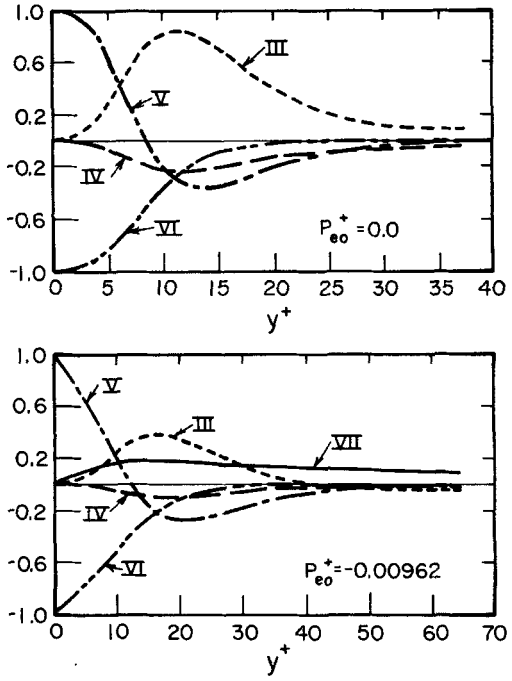

Figure 10. Kinetic energy balance for mean flow.
Ordinate made dimensionless with wall parameters

be consistent with Eqs. 30 and 32, terms I and II are combined into the single term,

$$\underset{\text{VII}}{-\bar{U}\frac{d\bar{\tau}}{dy}}=-\underset{\text{I}}{\left(\bar{U}\bar{U}\frac{\partial \bar{U}}{\partial x}+\bar{U}\frac{\partial \bar{U}}{\partial y}\right)}\underset{\text{II}}{-\bar{U}\frac{\partial \bar{P}}{\partial x}} \quad (44)$$

which represents the portion of the energy associated with the pressure gradient that does not go into accelerating the mean flow.

A comparison of the terms in the mean flow energy balances for the cases of $P^+_{eo}=0$ and of $P^+_{eo}=-0.00962$ is given in Figure 10. Integrals of the terms from the wall to y^+ are given in Figure 11. Term VII is zero if $P^+_{eo}=0$. In this case the viscous wall region receives mean flow energy from the outer flow in an amount equal to the integral of III over the region 0 to y^+_o. Term V redistributes mean flow energy and does not cause either a net increase or decrease in the viscous wall layer. Therefore the net effect of the mean flow energy that diffuses into the viscous wall region is to supply energy needed to generate turbulence, term IV, and to satisfy the direct viscous dissipation by the mean flow, term VI.

For $P^+_{eo}=-0.00962$ about two-thirds of the energy supply associated with the pressure gradient goes into accelerating the flow. The remainder, term VII, makes a contribution approximately equal to the turbulent diffusion, term III. The interesting aspect of these balances is that the large favorable pressure gradient causes a reduction of the turbulent diffusion of mean flow energy into the viscous wall layer. However, this is compensated by the energy supplied by the pressure gradient, so that the total energy supplied to the mean flow in the viscous wall layer is approximately the same for $P^+_{eo}=0$ and for $P^+_{eo}=-0.00962$. The mean flow energy directly dissipated by viscosity is slightly greater for $P^+_{eo}=-0.00962$ than for $P^+_{eo}=0$. Thus the generation

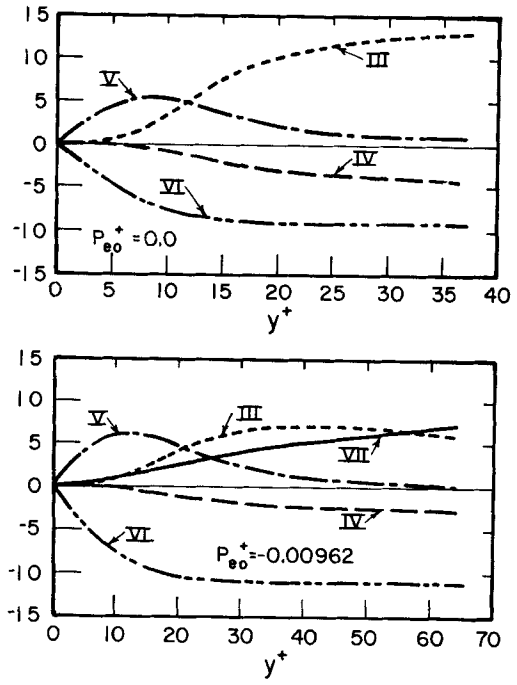

Figure 11. Integrals from 0 to y^+ of terms in kinetic energy balance for mean flow.
Ordinate made dimensionless with wall parameters

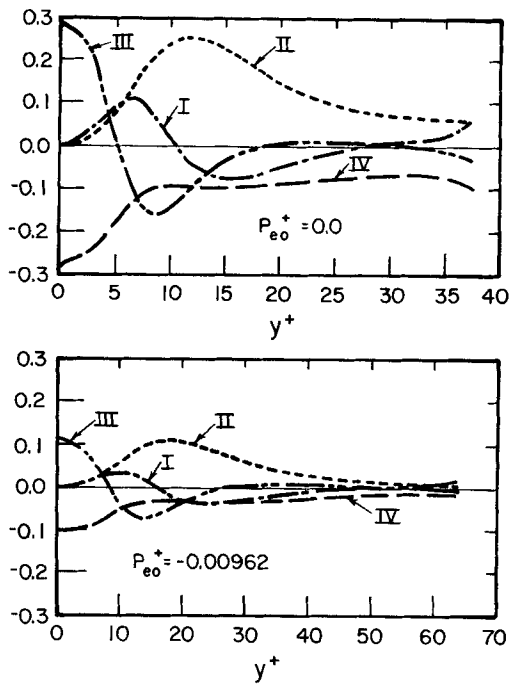

Figure 12. Kinetic energy balance for fluctuating velocity field.
Ordinate made dimensionless with wall parameters

of turbulence in the viscous wall layer for $P_{eo}^+ = -0.00962$ is somewhat smaller than for $P_{eo}^+ = 0$, but quite significant considering that this corresponds to a condition close to laminarization.

The equation for the total kinetic energy of the fluctuating velocities in a boundary layer is as follows:

$$0 = \underbrace{-\frac{\partial}{\partial y}\left[\overline{v\left(p+\frac{q^2}{2}\right)}\right]}_{\text{I}} \underbrace{-\overline{uv}\frac{\partial \bar{U}}{\partial y}}_{\text{II}} + \underbrace{\nu\frac{\partial^2}{\partial x_j \partial x_j}\left(\frac{\overline{q^2}}{2}\right)}_{\text{III}} \underbrace{-\nu\overline{\frac{\partial u_i}{\partial x_j}\frac{\partial u_j}{\partial x_j}}}_{\text{IV}} \quad (45)$$

Terms I and III are transfer terms that redistribute the turbulent kinetic energy between different regions of the flow. Term I represents the convective diffusion by turbulence of the turbulent kinetic energy. Term III represents the viscous diffusion of turbulent kinetic energy. Term II represents the production of turbulent kinetic energy by the mean flow energy. This term is exactly the same as term IV in Eq. 43 except that it is of opposite sign. Term IV is the dissipation that would occur in an isotropic field. It is used here instead of the true dissipation because this formulation allows for straightforward physical interpretation of the viscous terms.

The calculated turbulent kinetic energy balance is shown in Figure 12. Here, all terms are made dimensionless with ν and a friction velocity defined with the wall shear stress. The production of the turbulent kinetic energy is large throughout the viscous wall region. The production curve for $P_{eo}^+ = 0$ reaches a maximum of 0.25 at $y^+ = 12$. This is expected since the production is the product of the turbulent and viscous stresses, whose sum is equal to 1 in wall variables. This means that the product is maximized when the two stresses are equal to each other and attain the value of 0.5 in wall units. At the wall the dissipation is equal to the viscous diffusion of the turbulent kinetic energy. Dissipation is fairly large throughout the viscous wall region. The effect of the favorable pressure gradient, $P_{eo}^+ = -0.00962$, is to reduce the magnitudes of all the terms. However, no dramatic changes are observed in the relative importance of the different terms in the kinetic energy balance. Furthermore, as can be seen from Figure 13, the total net production of turbulence in the viscous wall region is roughly the same for $P_{eo}^+ = 0$ and for $P_{eo}^+ = -0.00962$. This turbulence diffuses into the region outside the viscous wall layer, where a net dissipation occurs.

Discussion

Summary of results

This paper uses scaling relations and the 2½D model of Nikolaides to provide an understanding of how favorable pressure gradients affect turbulence characteristics of the viscous wall layer. Favorable pressure gradients cause an acceleration of the fluid and a decrease of the shear stress with distance away from the wall. It is argued that the effect on turbulence is felt mainly through this shear stress variation. Shear gradients affect turbulence in the viscous wall region by acting as a source term in the streamwise momentum equation and by changing the flow at y_o^+.

The scaling relations developed depend on the assumption that y_o^+ is located at the inner edge of a log-layer, which has properties defined by Eqs. 6, 8, and 9. The principal result is that magnitudes of the fluctuating velocities, time parameters, and spatial parameters at y_o scale with the local shear stress rather

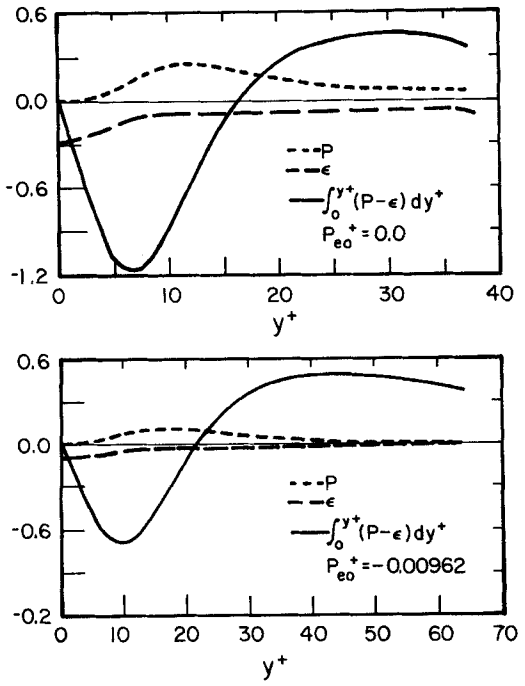

Figure 13. Effect of pressure gradient on net production of turbulence from 0 to y^+.
Ordinate made dimensionless with wall parameters

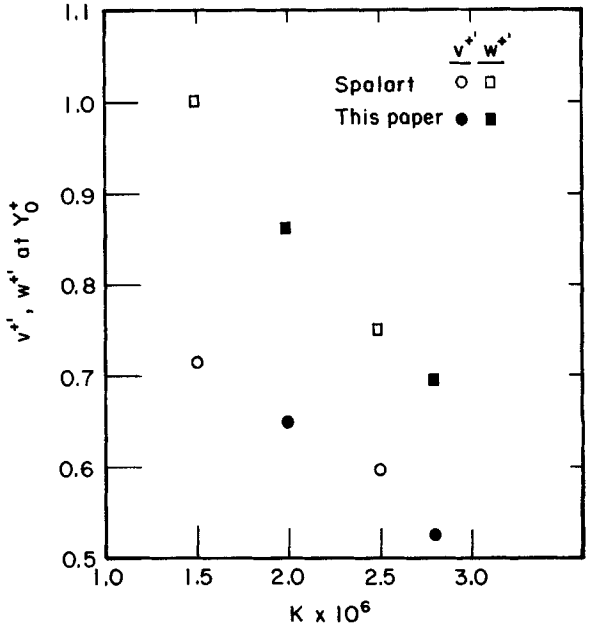

Figure 14. Scaling relations compared with computer experiments of Spalart (1986).

than the wall shear stress. Available laboratory measurements are used to argue that phase relations at y_o are unchanged in the presence of a favorable pressure gradient.

Good agreement is noted between the calculated velocity field and measurements. The calculated large influence of K on the v and w velocity components, shown in Figure 7, could have been anticipated from the scaling relations, which predict that v^+ and w^+ decrease at y_o^+ with increasing K.

The magnitude and location of the maximum in u^+ seem to determine the character of the u^+ vs. y^+ curves. Consequently, as can be seen from Figure 6, the decrease of u^+ at y_o^+ with increasing K^+ has only a small influence. The large effect of K on the Reynolds stresses, shown in Figure 9, is a consequence of the decrease in v^+. The calculated small effect of K on the Reynolds stress coefficient also could have been anticipated since the scaling relations required that this coefficient be independent of K at y_o^+.

The most interesting result from calculations with the 2½D model is the determination of the influence of the shear stress variation on the energy balances. The pressure gradient provides a direct source of energy to the viscous wall layer through the $d\tau/dy$ term. However, this seems to be balanced by a decrease of the diffusion of mean flow energy so that the net transfer of mean flow energy to the viscous wall region is approximately the same for a flow with zero pressure gradient and for flows with large enough favorable pressure gradients that they are close to relaminarization, Figure 11.

The mean flow energy is directly dissipated by viscosity and is used to produce turbulence. As can be seen from Figure 11, the total production of turbulence (when scaled with the wall shear stress and kinematic viscosity) is approximately the same for a zero pressure gradient and for a large favorable pressure gradient. The total dissipation of turbulence in the viscous wall region is also nearly the same. This leads to the interesting result, shown in Figure 13, that the net total production of turbulence in the viscous wall region is roughly the same for a zero pressure pressure gradient and for a large favorable pressure gradient. Since there is a net dissipation of turbulent energy in the region $y^+ > y_o^+$, it is necessary that net production in the viscous wall region remain positive in order for the turbulence to be sustained. The calculated results therefore indicate that the turbulence production process does not deteriorate provided that the scaling arguments remain correct. This suggests that laminarization is related to a breakdown of the scaling arguments.

Relaminarization

It is therefore of interest to understand the physical significance of the finding that the minimum value of P_{eo}^+ (for which scaling relations hold) corresponds closely to the conditions for relaminarization found in laboratory experiments.

From Figure 2 it can be seen that $C_f/2$ is a constant for moderate and large favorable pressure gradients. Therefore, from Eq. 27, it is concluded that the upper branches of the curves in Figure 1 correspond to a region where the mean velocity profile increases more rapidly than P^+ decreases. This observation might provide a sufficient physical interpretation since it agrees with the study of Patel and Head (1968) which showed that a rapid increase of the mean velocity is a sign of imminent relaminarization.

However, as indicated in the previous section, it is also of interest to examine how the scaling arguments might break down. This could occur because of the disappearance of the log-layer, since the scaling assumes y_o is located in the log-layer. It also could occur because the characteristic Reynolds number of the outer flow becomes so small that the net dissipation of turbulent energy in the region $y^+ > y_o^+$ is much larger than what is predicted from scaling relations developed for high Reynolds number flows. A criterion developed by Bradshaw (1969) seems to address this issue.

Bradshaw defined an eddy Reynolds number as $\ell(\tau/\rho)^{1/2}/\nu$, where ℓ is the dissipation length parameter defined by Eq. 9. He argued that when this is too small turbulence cannot exist. In the log-layer, $\ell = \kappa y$. Beyond the log-layer, $y > 0.2\delta$, a good approximation is that $\ell = 0.2\kappa\delta$.

In a zero pressure gradient flow the maximum eddy Reynolds number occurs at the outer edge of the log-layer. For flows with large favorable pressure gradients $\tau(y)$ decreases with y so the maximum value of the eddy Reynolds number occurs somewhere in the log-layer. According to Bradshaw, laminarization will occur when the maximum is at the outer edge of the viscous wall region; that is,

$$\left| \frac{(\tau/\rho)^{1/2} y}{\nu} \right|_{\max} = y_o^o \tag{46}$$

The derivative of the eddy Reynolds number with respect to y provides the following criterion for a maximum:

$$\tau^+ + \frac{d\tau^+}{dy^+}\frac{y^+}{2} = 0 \tag{47}$$

Substituting Eq. 1 for τ^+ gives

$$\left| \frac{(\tau/\rho)^{1/2} y}{\nu} \right| = \frac{-(\tau/\tau_w)^{1/2}}{Pe^+ + \frac{1}{2}\frac{d\tau^+}{dy^+}} \tag{48}$$

at a maximum. Now if the maximum occurs at edge of the viscous wall layer it is necessary that

$$y_o^o = 40 = \frac{-\tau_o^{+1/2}}{Pe_o^+ + \frac{1}{2}\left(\frac{d\tau^+}{dy^+}\right)_o} \tag{49}$$

This shows that the criterion of a maximum eddy Reynolds number at the edge of the viscous wall region is satisfied at the minimum of $P_{eo}^+ = -0.00962$, where $P_{eo}^+ = (d\tau^+/dy^+)_o$ and $\tau_o^+ = 0.333$.

Comparison with direct numerical simulation

During the review of this manuscript a recent paper on the direct numerical simulation of sink flow boundary layers (Spalart, 1986) was called to our attention.

These new experimental results provide additional support to the scaling used in this paper. Spalart finds a correlation coefficient for the Reynolds stress at y_o^+, equal to 0.5, that is approximately the same for $K = 0$, 1.5×10^{-6}. This is consistent with the experimental results of Badri Narayanan and Narasimha (1974) and with the assumption made in this paper that the phases of the velocity components at y_o^+ remain unchanged. The influence of K on the maximum values of w^+ and v^+ computed by Spalart are compared in Figure 11 with the values at y_o^+ obtained from scaling arguments. The good agreement supports the result that turbulence quantities at y_o^+ are unchanged if they are scaled with a friction velocity based on the local shear stress. The energy balances as well as Figure 9 of the Spalart paper support Eq. 8, used in developing the scaling relations.

The numerical experiments show that a turbulent boundary layer cannot be sustained at $K = 3.0 \times 10^{-6}$ but can be sustained at $K = 2.5 \times 10^{-6}$. This agrees with present laboratory measurements and the value of $K = 2.8 \times 10^{-6}$ obtained if one uses the minimum P_{eo}^+ as a criterion.

Figure 13e of the Spalart paper gives a balance of $\overline{q^2}$, for $K = 1.5 \times 10^{-6}$. This can be compared with the balance of $\overline{q^2}/2$ shown in Figure 12 of this paper if the terms in the energy balance are divided by two. Good, but not exact, agreement is noted. Both investigations show a change in the magnitudes, but not in the relative values of the terms in the energy balance with increasing K.

Acknowledgment

This work has received support from the Office of Naval Research under Project No. NR 657-728 and from the Shell Companies Foundation.

Notation

C_f = skin friction coefficient
ℓ = characteristic length of large eddies
P = pressure
P^+ = dimensionless pressure gradient, Eq. 25
P_e = effective pressure gradient
q = characteristic turbulent velocity
t = time
T = period
T_B = bursting period
u = fluctuating streamwise velocity
u_w^* = friction velocity $= (\tau_w/\rho)^{1/2}$
U = streamwise velocity
U_∞ = free stream velocity
V = velocity component normal to wall
v = fluctuating normal velocity component
w = fluctuating spanwise velocity component
W = velocity component in spanwise direction
x = coordinate in flow direction
y = coordinate normal to wall
y^+ = dimensionless y ($y^+ = yu^*/\nu$)
z = coordinate in spanwise direction

Greek letters

Δ_τ = shear stress gradient parameter
ϵ = dissipation
κ = von Karman constant = 0.41
Φ_i = phase of velocity component i
λ = streak spacing
λ_g = Taylor microscale
μ = molecular viscosity
ν = kinematic viscosity
ρ = density of fluid
τ = shear stress
τ_w = wall shear stress

Subscripts

o = quantity located at outer edge of viscous wall region
w = evaluated at wall
1 = quantity associated with inner eddies
2 = quantity associated with outer eddies

Superscripts

$+$ = nondimensional with friction velocity, u^*, and kinematic viscosity
o = quantity scaled with shear stress at outer edge of viscous wall region and assumed constant independent of acceleration

Other symbols

$\overline{\quad}$ = time average
$|\hat{}|$ = amplitude

Literature Cited

Back, L. H., and R. A. Seban, "Convective Heat Transfer in a Convergent-Divergent Nozzle," *Proc. Heat Trans., Fluid Mech. Inst.*, **20,** 410 (1967).

Badri Narayanan, M. A., and V. Ramjee, "On the Criteria for Reverse Transition in a Two-dimensional Boundary Layer Flow," *J. Fluid Mech.*, **35,** 225 (1969).

Badri Narayanan, M. A., and R. Narasimha, Rept. No. 74 FM-15 Dept. Aero. Eng. Ind. Inst. Sci., Bangalore (1974). [See Narasismha, R. L., and K. P. Sreenisasan, "Relaminarization of Fluid Flows," *Adv. Appl. Mech.*, **19,** 221 (1979)].

Bradshaw, P., "A Note on Reverse Transition," *J. Fluid Mech.*, **35,** 387 (1969).

———, "Turbulence," *Topics in Applied Physics*, v. 12, Springer-Verlag, Berlin (1976).

Eckelman, L. D., G. Fortuna, and T. J. Hanratty, "Drag Reduction and the Wavelength of Flow-Oriented Wall Eddies," *Nature*, **236,** (67), 94 (1972).

Finnicum, D. S., "Pressure Gradient Effects in the Viscous Wall Region of a Turbulent Flow," Ph.D. Thesis, Univ. Illinois, Urbana (1986).

Fortuna, G., and T. J. Hanratty, "The Influence of Drag-Reducing Polymers on Turbulence in the Viscous Sub-Layer," *J. Fluid Mech.*, **53,** 575 (1972).

Hatziavramidis, D. T., and T. J. Hanratty, "The Representation of the Viscous Wall Region by a Regular Eddy Pattern," *J. Fluid Mech.*, **95,** 655 (1979).

Hinze, J. O., Turbulence, McGraw-Hill, New York, 2nd ed. (1975).

Hogenes, J. G. A., and T. J. Hanratty, "The Use of Multiple Wall Probes to Identify Coherent Flow Patterns in the Viscous Wall Region," *J. Fluid Mech.*, **124,** 363 (1982).

Jones, W. P., and B. E. Launder, "Some Properties of Sink-Flow Turbulent Boundary Layers," *J. Fluid Mech.*, **56,** 337 (1972).

Julien, H. L., W. M. Kays, and R. J. Moffat, "The Turbulent Boundary Layer on a Porous Plate: Experimental Study of the Effects of a Favorable Pressure Gradient," Stanford Univ. Thermosci. Div. Tech. Rept. HMT-4 (1969).

Kline, S. J., W. C. Reynolds, F. A. Schraub and P. W. Runstadler, "The Structure of Turbulent Bounding Layers," J. Fluid Mech., **30,** 741 (1967).

Launder, B. E., "The Turbulent Boundary Layer in a Strongly Negative Pressure Gradient," Rept. No. 71, Gas Turbine Lab., Mass. Inst. Tech., Cambridge (1963).

——, "Laminarization of the Turbulent Boundary Layer by Acceleration," Rept. No. 77, Gas Turbine Lab., Mass. Inst. Tech., Cambridge (1964).

Launder, B. E., and W. P. Jones, "A Note on Bradshaw's Hypothesis for Laminarization," ms. 69-HT-12, *ASME-AIChE Heat Trans. Conf.*, Minneapolis (Aug. 1969).

Launder, B. E., and H. S. Stinchcombe, "Non-Normal Similar Turbulent Boundary Layers," Imp. Coll. Note TWF/TN 21 Dept. Mech. Eng. London, England (1967).

Loyd, R. J., R. J. Moffat, and W. M. Kays, "The Turbulent Boundary Layer on a Porous Plate: An Experimental Study of the Fluid Dynamics with Strong Favorable Pressure Gradient and Blowing," Stanford Univ. Thermosci. Div. Tech. Rept. MMT-13 (1970).

Moretti, P. H., and W. M. Kays, "Heat Transfer to a Turbulent Boundary Layer with Varying Free-Stream Velocity and Varying Surface Temperature—An Experimental Study," *Int. J. Heat Trans.*, **8,** 1187 (1965).

Nikolaides, C., "A Study of the Coherent Structures in the Viscous Wall Region of a Turbulent Flow," Ph.D. Thesis, Univ. of Illinois, Urbana (1984).

Nyden, O. B., "A Study of Coherent Structures in a Turbulent Boundary Layer and Effects of Favorable Pressure Gradients," Thesis, Chalmers Univ. of Technol., Dept. Appl. Thermodynam. and Fluid Mech., Göteborg, Sweden (1985).

Patel, V. C., "Calibration of Preston Tube and Limitations of Its Use in Pressure Gradients," *J. Fluid Mech.*, **23,** 185 (1965).

Patel, V. C., and M. R. Head, "Reversion of Turbulent to Laminar Flow," *J. Fluid Mech.*, **34,** 371 (1968).

Pohlhausen, K., "Zur näherungsweisen Integration der Differentialgleichung der laminaren Reibungschicht," *Z.A.M.N.*, **1,** 252 (1921).

Sandborn, V. A., and R. J. Slogar, "Study of the Momentum Distribution of Turbulent Boundary Layers in Adverse Pressure Gradients," NACA TN-3264 (1955).

Spalart, P. R., "Numerical Study of Sink-Flow Boundary Layers," *J. Fluid Mech.*, **172,** 307 (1986).

Tennekes, H., and J. L. Lumley, *A First Course in Turbulence*, MIT Press, Cambridge (1972).

Townsend, A. A., "Equilibrium Layers and Wall Turbulence," *J. Fluid Mech.*, **11,** 97 (1961).

———, *The Structure of Turbulent Shear Flow*, 2nd ed., Cambridge (1976).

Manuscript received Feb. 23, 1987, and revision received Oct. 12, 1987.